Available online at www.sciencedirect.com
ScienceDirect
Catalysis Today 133–135 (2008) 174–180
CATALYSIS TODAY
www.elsevier.com/locate/cattod

An investigation of the activation process of high temperature shift catalyst

Morgana Scariot [a,b], Maria Suzana P. Francisco [a], Maura H. Jordão [a], Daniela Zanchet [a,*], Marco A. Logli [c,d], Valéria P. Vicentini [d]

[a] *Laboratório Nacional de Luz Síncrotron, CP 6192, 13083-970 Campinas, SP, Brazil*
[b] *Universidade Federal do Rio Grande do Sul, 90040-060 Porto Alegre, RS, Brazil*
[c] *Universidade de São Paulo, Dep. Química, CP 26077, 05599-970 São Paulo, SP, Brazil*
[d] *Oxiteno S.A. Ind. E Com., Av. Ayrton S. da Silva 3001, 09380-440 Mauá, SP, Brazil*

Available online 14 February 2008

Abstract

The aim of this work is to address the activation process of a high temperature shift (HTS) catalyst, composed of $Fe_2O_3/Cr_2O_3/CuO$, by analyzing it before activation (HTS-V) and after activation (HTS-A) using complementary characterization techniques. The textural and morphological characterizations were done by transmission electron microscopy (TEM) and nitrogen physisorption at 77 K; crystallographic structure was confirmed by X-ray diffraction (XRD); electronic structure was analyzed by X-ray absorption spectroscopy (XAS) and the chemical composition of the catalyst's surface was obtained by X-ray photoelectron spectroscopy (XPS). The investigation pointed out that the HTS-V catalyst presents good textural and morphological properties, which are not deeply affected by the activation process (sample HTS-A). The iron oxide phase in the HTS-V catalyst is hematite whereas in HTS-A catalyst is magnetite with Fe^{2+}/Fe^{3+} ratio close to the expected value (0.5). For both samples, the Cr ions seem to be incorporated in the iron oxide lattice with higher concentration at particle surface. In the HTS-V catalyst, the Cu ions have oxidation number II and occupy in average distorted octahedral sites; after the activation, the Cu ions are partially reduced, suggesting that the reduction of the Cu species is complex.

Keywords: WGSR; HTS; Catalyst; XAS

1. Introduction

In the process to produce hydrogen or synthesis gas it is usual to have a step where takes place the carbon monoxide conversion, the so-called water gas shift reaction (WGSR), or directly shift reaction. The carbon monoxide conversion to carbon dioxide under high temperature in the presence of steam is a reversible and exothermic reaction [1,2]:

$$CO(g) + H_2O \rightleftarrows CO_2(g) + H_2(g)\ \Delta H = -40.6\ \text{kJ mol}^{-1} \quad (1)$$

This reaction is a relevant step in many industrial processes, such as ammonium and hydrogen productions with high degree of purity [1,2]. The reaction maximizes the hydrogen generation from steam reforming of natural gas or nafta, and at the same time removes the residual carbon monoxide that acts as poison for the most sensitive catalysts. To obtain economically acceptable conversions, the reaction is carried out in two stages. The first one is performed in the temperature range of 320–420 °C under favorable kinetic conditions, known as HTS reaction (high temperature shift); the second one, called LTS reaction (low temperature shift), takes place at temperature around 200 °C in such way to be thermodynamically favorable.

The industrial HTS catalyst is mainly composed of iron oxide particles with the addition of promoters such as chromium and copper. It is usually commercialized as hematite (α-Fe_2O_3), that is converted *in situ* to magnetite (Fe_3O_4) during the activation process, which is the iron active phase in the HTS reaction. It is also possible to find catalysts in the form of γ-Fe_2O_3 (maghemita) and α-FeOOH (goethita); the type of initial iron oxide is known to affect the final textural properties of the activated catalyst [3,4]. The activation process is a critical step

* Corresponding author. Tel.: +55 19 3512 1010; fax: +55 19 3512 1004.
E-mail address: zanchet@lnls.br (D. Zanchet).

0920-5861/$ – see front matter © 2007 Elsevier B.V. All rights reserved.
doi:10.1016/j.cattod.2007.12.090

and requires a careful control of the reduction conditions to lead to the best catalytic performance. During the reduction and subsequent reaction conditions, the catalysts must not be exposed to hydrogen in the lack of steam to avoid the formation of metallic iron that would lead to undesirable/parallel reactions.

Under HTS conditions, pure magnetite catalyst rapidly sinters and loses its activity [3,5]. The addition of chromia leads to a better resistance against sintering and as a consequence against the decrease of surface area, acting as a textural promoter [3,5,6]. Although the highest sintering resistance is obtained when chromia concentration is around 14 wt.% [4,6], the best compromise is achieved with concentration of 8–10 wt.%. At these lower values, there is an optimization of both the textural properties and intrinsic activity (activity per unit of surface area of the catalyst). This balance must be taking into consideration because Cr(III) replaces active Fe(III)/Fe(II) octahedral sites [5,7] and at higher concentration, there is a drawback concerning the loss of intrinsic activity [6].

Copper oxide has also been used as promoter for HTS catalysts, providing a final material with superior selectivity and catalytic performance than the pure mixed oxide Fe_2O_3/Cr_2O_3 [3,7–9]. It is important to note, however, that both promoters are necessary since only Fe_2O_3/CuO has smaller intrinsic activity than pure Fe_2O_3 [7,9]. A good balance was found for a composition of Fe_2O_3 (88–91 wt.%), Cr_2O_3 (7–10 wt.%), and CuO (2–3 wt.%). Two other interesting aspects of using CuO as promoter is the decrease of more than 20% in the activation energy when compared to the Fe_2O_3/Cr_2O_3 catalyst in the same conditions and the possibility to reduce the temperature required for activation, what is interesting for decreasing sintering effects and for adopting a low cost industrial procedure [5]. It is important to point out, however, that the understanding of the actual role of the copper oxide promoter is not a simple task considering its small concentration and the restricted number of techniques that can be employed in such case. In fact, it remains to be fully understood its participation as a real active site or as an indirect agent, by modifying the iron electronic structure.

Apart the extensive work in the literature about HTS catalysts, the results are not usually straightforward comparable nor related in a simple way due to the differences in the type and morphology of the initial iron oxide particles and the operational conditions. In general, it has been shown that the morphological/textural, structural and electronic properties of HTS catalyst and as a consequence its performance may depend on several parameters [5,6,8,10]. A detail characterization of the target catalyst under operational conditions is then required to succeed in its optimization. Equally important is to explore the combination of several and complementary characterization techniques. As an example, investigations that consider only the structural properties and catalytic performance negligence the sintering process that decrease the surface area and may be highly dependent on the particle morphology. On the other hand, a high focus in the morphological/textural properties can be insufficient in explaining the catalytic behavior due to the lack of information about the electronic state of the iron ions. The role of structural and electronic characterizations resides in obtaining complementary information, such as, the insertion of copper and chromium in the iron oxide lattice [7,8,10,11], the presence of metallic copper as electronic modifier of Fe_2O_3/Cr_2O_3 system [8], the copper/chromium enrichment near the surface [7,5,10], that, together with textural characterization and catalytic results, have been suggesting a synergism of the elements. Therefore, the overall findings from morphological/textural, structural and electronic studies are fundamental to achieve a better understanding of the particular HTS system.

In the present work, we studied a HTS catalyst (90 wt.% Fe_2O_3, 8 wt.% Cr_2O_3, and 2 wt.% CuO) synthesized by Oxiteno S.A. Ind. E Com. (Brazil), aiming to understand the morphological, textural, structural, and electronic modifications after the activation process. To accomplish this goal, the catalyst was analyzed before activation (HTS-V catalyst) and after activation (HTS-A catalyst) and different characterization techniques were carefully chosen. The morphological/textural features were analyzed by transmission electron microscopy (TEM) and nitrogen physisorption at 77 K. Crystallographic structure was confirmed by X-ray diffraction (XRD). X-ray absorption spectroscopy (XAS) was used to probe the local environmental of Fe, Cr and Cu ions given information about site occupancy and electronic state. X-ray photoelectron spectroscopy (XPS) was employed to probe the surface composition of the HTS catalysts, which could be compared to expected bulk values.

2. Experimental

2.1. Synthesis method and catalytic activity

The catalysts before activation and after activation, denominated HTS-V and HTS-A, respectively, were synthesized by Oxiteno S.A. Ind. E Com. The catalysts were prepared by precipitation techniques at room temperature using analytical grade reagents, followed by heating at 500 °C for 2 h under nitrogen flow (100 ml/min). The catalytic activation and performance were evaluated using 12 ml of powder within −20 and +32 mesh size in a fixed bed microreactor consisted of a stainless tube. All experiments were carried out under isothermal conditions by adapting the procedure proposed by Chinchen et al. [12], where a special procedure is used to accelerate the initial decay of the activity to obtain a catalyst in the steady-state. The conditions were: H_2/CO/CO_2 as gas feeding = 80/10/10% (v/v/v), steam/gas molar ratio = 0.4, steam/carbon molar ratio = 3.6, gas hourly space velocity (GHSV) = 14,000 h^{-1} and pressure = 25 kgf/cm^2. The CO conversion after the activation process was 58% at 350 °C, similar to the performance of a commercial reference catalyst under the same test conditions.

2.2. Textural analysis

The isotherms of N_2 adsorption at 77 K were obtained using Micromeritics TriStar 3000 v.4.00 model equipment. Before the measurements, the samples were degassed at 200 °C under

low pressure 16.7×10^3 Pa (outgased). Complementary data was acquired in a mercury porosimetry also from Micromeritics.

2.3. TEM images

The TEM images were obtained in a JEM-3010 microscope operating at 300 kV and 0.17 nm point resolution at the laboratory of electron microscopy at the Brazilian Synchrotron Light Laboratory (LNLS) in Campinas, SP, Brazil. The powder was ultrasonically suspended in isopropyl alcohol and the suspension deposited on an amorphous carbon coated nickel grid. Qualitative chemical analysis by energy dispersive X-ray spectroscopy (EDS) was used to identify the existence of phase segregation of the promoters (chromia and copper oxide). A 10 nm probe has been used in this work.

2.4. XRD data

The X-ray powder diffraction patterns were obtained at XRD1-LNLS beamline using $\lambda = 0.17705$ nm, 2θ in the 20–110° range, step size of 0.04° and 3.0 s/step. The identification of crystalline phases was obtained by comparison with JCPDS files.

2.5. XAS analysis

The XAS spectra were acquired in the XAFS1-LNLS beamline for Fe, Cr and Cu K-edges. The samples were prepared as membrane or pressed powder and the measurements were done in transmission mode. In this work we mainly focused in the near edge structure of the XAS spectra (XANES region).

2.6. XPS measurements

The XPS measurements were performed in a homemade UHV chamber ($\sim 9 \times 10^{-9}$ mbar), using Al Kα (1486.6 eV; 10 kV and 18 mA) and a hemispheric spectrometer from SPECS (PHOIBOS150 HSA3500 with nine single channel electron multipliers) with pass energy of 40 eV. The powder samples were analyzed without further treatment. The XPS binding energies were referenced to the C 1s at 284.8 eV from the sample-holder. The curve-fittings had mixings of Gaussian/30%–Lorenzian lineshapes, and Shirley function as background [13]. The sensitivity factors for quantitative analysis were referenced to $S_{C\ 1s} = 1.0$. The spectra were analyzed using CasaXPS software [14], version 2.2.99.

3. Results and discussion

The HTS-V catalyst presented adsorption isotherm that resemble a macroporous material, where the amount of adsorption tends to infinite for P/P_0 value tending to 1 (Fig. 1). However, some different aspects can be found such as the measurable volume absorbed up to $P/P_0 \sim 0.8$ due to a monolayer completion and a significant adsorbed volume at $P/P_0 \rightarrow 1.0$ (200 cm g^{-1}), indicating the existence of a fraction of mesoporous (2–50 nm of diameter) in the HTS-V catalyst. This was confirmed by mercury porosimetry that pointed out 75% of the porous diameter in the range of 10–50 nm. The hysteresis curve presented in Fig. 1 is characterized by two branches of asymptotic isotherm relative to the vertical position (type H3). This behavior is associated to the presence of particles added not rigid in plate form, originating pores in crack. The results of specific surface area (S_{BET}), pore volume, and average pore diameter are shown in Table 1.

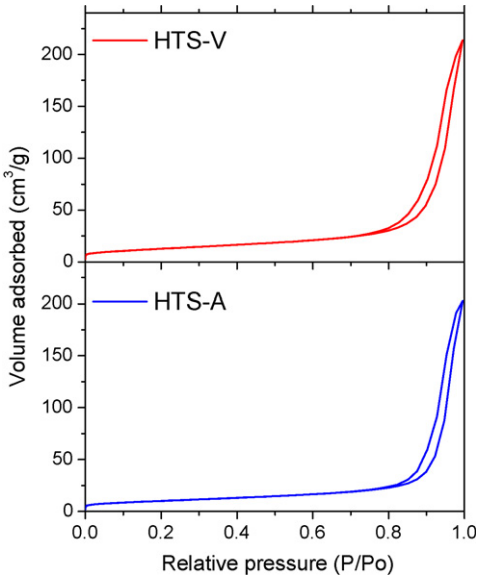

Fig. 1. N_2 adsorption at 77 K of HTS-V and HTS-A catalysts.

After the reaction, the HTS-A catalyst showed a similar adsorption isotherm and a small decrease in the S_{BET} value (Fig. 1 and Table 1). The porous volume and average pore diameter did not change very much after the activation, what are directly related to the porous size distribution. These are excellent results considering that most data presented in the literature point out a strong decrease of surface area after equivalent reaction conditions [4,5]. For example, Edwards et al. [5] studied a HTS catalyst ($Fe_2O_3/Cr_2O_3/CuO$) synthesized by co-precipitation method and found that after 1000 h under WGSR at 370 °C the surface area decrease more than 60%. Gonzalez et al. [15] studied a commercial Fe_2O_3/Cr_2O_3 system and found the decrease of 63% in the surface area after WGSR at 360 °C and the shifted of pore volume to higher value (from 0.23 to 0.28 $cm^3\ g^{-1}$) due to the blocking of the pores with smaller sizes (sintering process). Keiski et al. [16] found that when the catalytic activity decreases, the surface

Table 1
Values of specific surface area, porous volume, and average pore diameter obtained for HTS-V and HTS-A catalysts

Catalyst	HTS-V	HTS-A
Specific surface area (S_{BET}) ($m^2\ g^{-1}$)	44	33
Pore volume ($cm^3\ g^{-1}$)	0.28	0.26
Average pore diameter (nm)	22.4	26.6

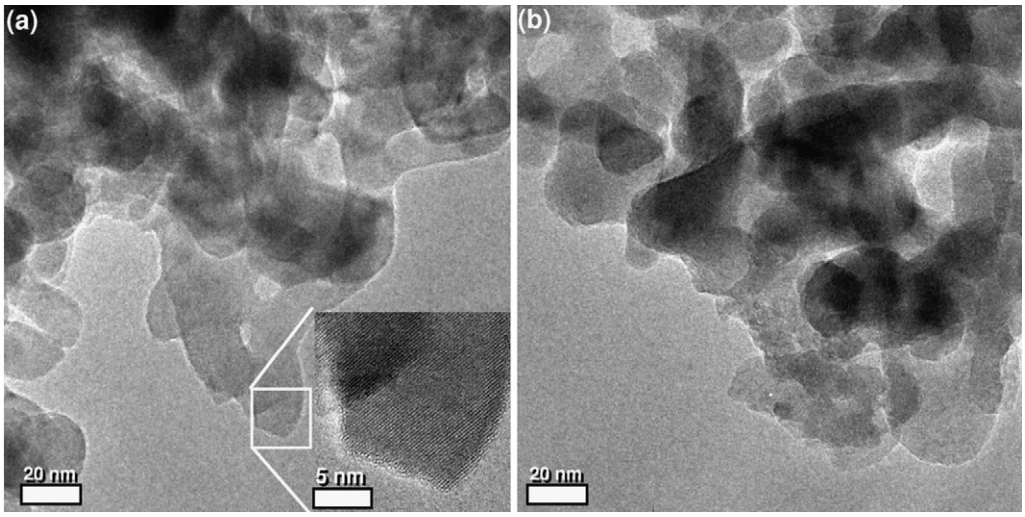

Fig. 2. TEM images of: (a) HTS-V and (b) HTS-A catalysts. The inset in (a) shows the high-resolution image of the marked area.

area of the catalyst decreases, the average pore radius increases, the total porous volume remains almost unchanged and the number of smaller pores decreases. Based on these results, they suggested that smaller pores (<30 nm) give the main contribution to the shift reaction. In our case, both HTS-V and HTS-A present mean pore size below 30 nm.

Fig. 2 presents the TEM images obtained for HTS-V and HTS-A catalysts. It is possible to note that before the activation, the HTS-V catalyst is composed of aggregates of elongated particles with sizes in the range of 20–30 nm (short axis) and a striking degree of interconnection (Fig. 2a). High-resolution TEM images (see inset in Fig. 2a) confirmed that the elongated particles are monocrystalline (the lattice fringes in the image corresponds to the (1 0 0) lattice planes of hematite, periodicity of 2.70 Å). The origin of the unusual degree of interconnection and the elongated morphology is still not understood but might indicate that the growth mechanism by ''oriented attachment'', where particles stick together with the same crystallographic orientation, could have been favored [17]. This mechanism has been found in other iron oxide systems with nanometric sizes. Further studies are necessary to corroborate this proposition.

Fig. 2b shows the TEM image of HTS-A catalyst. It can be seen that the main modification of the particles morphology after the activation seems to be the decrease of the interconnection degree and an increase of particle size. It is likely that the interconnected network has been broken with the activation and sintering has occurred. This may have lead to a more compact structure, which would be in agreement with the small decrease of the surface area of the HTS-A catalyst. A very important point to be noted is that both HTS-V and HTS-A catalysts present rather homogenous particle sizes. For example, the data presented by Edwards et al. [5] showed that in their case, the fresh activated catalyst already presented a very broad size distribution of irregular magnetite crystallites (range of 10–60 nm). Although not deeply tackled in the literature, the particle morphology should be a key parameter to be controlled in the HTS catalyst since the presence of a large number of small particles, which would contribute to an increase of surface area, would also favors the sintering process. In our case, the rather homogenous particle size and the elongated morphology of the HTS-V catalyst is likely to have played a major role to keep good textural properties after activation.

Concerning the chemical homogeneity of the particles, the EDS/TEM analysis did not point out clearly the formation of segregate phases of chromium or copper oxides in both catalysts, different from the work by Edwards et al. [5] where a tenorite phase (CuO, size of 12 nm) could be clearly identified. The 10 nm probe used in this work did not allow obtaining conclusive results about the enrichment of chromium or copper on the surface of individual iron oxide particles, which has been addressed by XPS analysis (see below).

Fig. 3 presents the XRD results. It shows that the HTS-V catalyst corresponds to hematite, whereas the HTS-A catalyst corresponds to magnetite, the active phase. Segregated crystalline phases of copper or chromium oxides were not detected in the XRD patterns. Both results agree well with the information obtained by TEM.

To obtain a deeper knowledge about the catalysts structure and activation process XANES experiments were performed to probe the three elements, iron, chromium and copper. The XANES spectrum depends on both the symmetry and chemical environment of the absorbing atom. As a consequence, it is possible to probe not only the iron environment but also the chromium and copper ones, complementary.

The XANES spectra of Fe K-edge of HTS-V and HTS-A catalyst are presented in Fig. 4a and points out the modification of the iron environment after the activation. Fig. 4b and c present the comparisons between the spectra of hematite reference compound and HTS-V catalyst and the spectra of magnetite reference compound and HTS-A catalyst, respectively. An excellent agreement between them could be observed, corroborating the XRD results.

Interesting features about the XANES spectrum of the Fe K-edge are the edge position (usually taken at the first derivative maximum) and the pre-peak intensity and position, at 7112 eV.

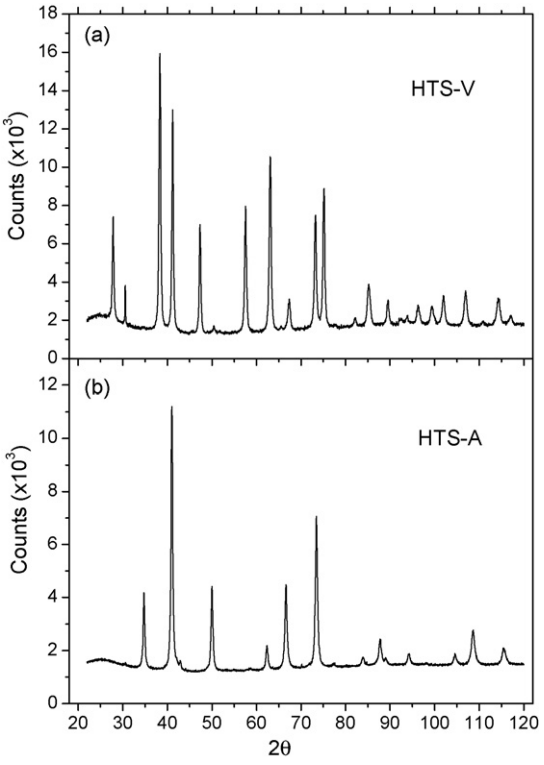

Fig. 3. XRD patterns of HTS-V and HTS-A catalysts. The peaks in (a) and (b) match the hematite (α-Fe_2O_3) and magnetite (Fe_3O_4) phases, respectively.

The edge position depends on the oxidation number while the pre-peak depends on both the oxidation number and the symmetry of the occupied sites. The shift of the edge energy can be understood in terms of the loss of the shielding electrons in higher oxidation states, which increases the ionization energy and shift the edge position to higher energy values. Concerning the pre-peak, the responsible transition for its appearing in the Fe K-edge is an electron transition from 1s → 3d sublevel, that is forbidden for a center-symmetric environment, such as a perfect octahedral site. However, this transition becomes possible because the mixing of the 3d–4p orbitals or a geometrical distortion of the original center-symmetric environment. Therefore, atoms in octahedral sites usually present a low intensity pre-peak [18]. For non-center-symmetric sites (tetrahedral sites, for example) there is an increase of pre-peak intensity [18]. It is known that in hematite the Fe^{+3} ions occupy octahedral sites while in the magnetite the Fe^{+3} ions occupy the octahedral sites and the Fe^{+2} ions occupy both octahedral and tetrahedral sites. This justifies the clear difference in the pre-peak intensity for the HTS-V and HTS-A catalysts (Fig. 4a).

It has been suggested that the Fe^{+2}/Fe^{+3} ratio may affect the HTS catalytic activity although some data in the literature show that this is not always the case [10]. A detailed analysis on the edge position or the pre-peak intensity in XANES spectrum can also provide the information on the Fe^{+2}/Fe^{+3} ratio and it has been explored in other Fe-based compounds [18,19]. In this work we used the methodology proposed by Capehart et al. [20] in which the absorption edge shift is obtained by the integration of the vacant electronic sites above the Fermi level. We found

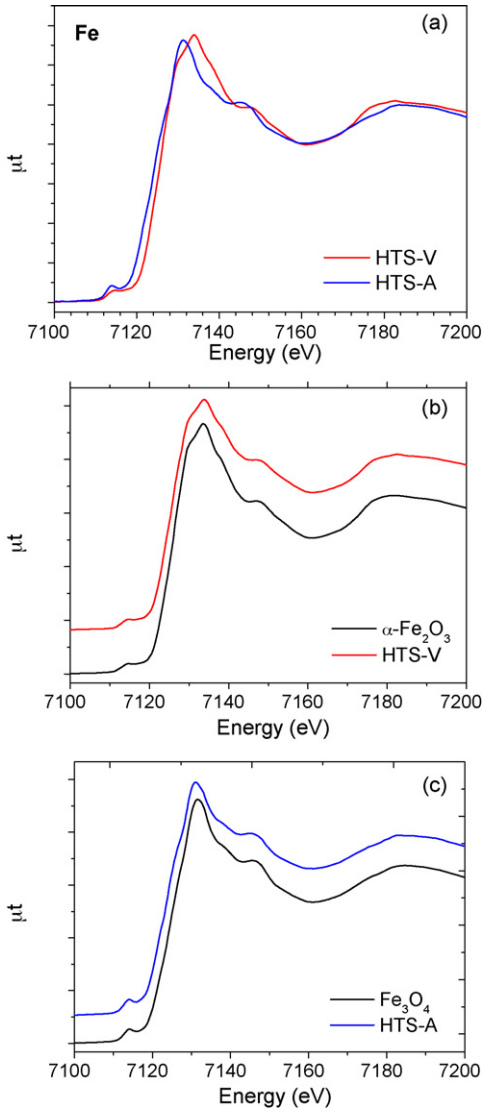

Fig. 4. XANES spectra of Fe K-edge of: (a) HTS-V and HTS-A catalysts and a comparison with the two reference compounds (b) hematite and (c) magnetite.

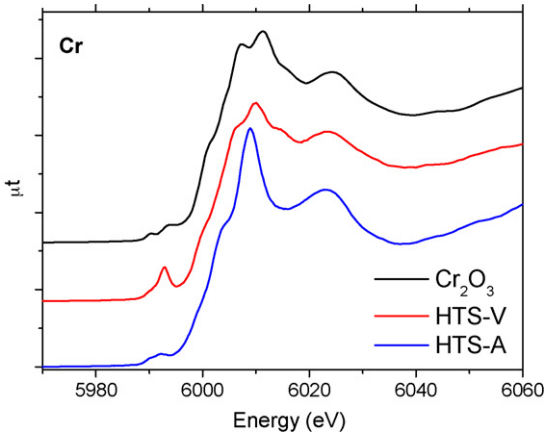

Fig. 5. XANES spectra of Cr K-edge of HTS-V and HTS-A catalysts compared to the Cr_2O_3 reference compound.

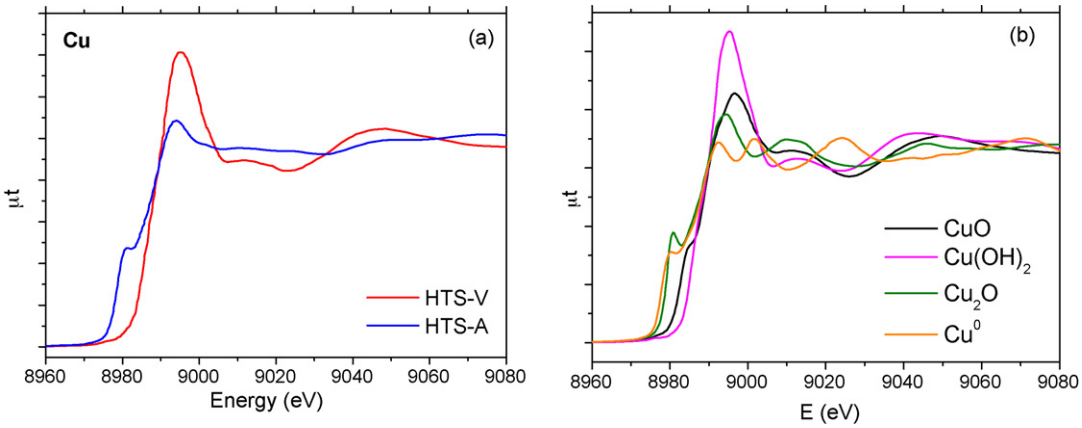

Fig. 6. XANES spectra of Cu K-edge of: (a) HTS-V and HTS-A catalysts and (b) reference compounds.

that the HTS-A catalyst present a Fe^{+2}/Fe^{+3} ratio similar to reference compound magnetite.

The Cr K-edge XANES spectra is shown in Fig. 5. It is clear that a major modification of the Cr environment takes places during activation. The HTS-V catalyst resembles the Cr_2O_3 reference compound spectrum, while HTS-A matches very well the ferrite $Fe_{3-x}Cr_xO_4$ spectra [21]. Analyzing the edge position we found that both HTS-V and HTS-A catalysts correspond to oxidation number III. As a result, the higher intensity of the pre-peak position of the HTS-V catalyst compared to the Cr_2O_3 reference compound is likely to be associated to a distortion of the octahedral site symmetry. This analysis in association with EDS/TEM and XRD results where no segregation of chromia phase was detected suggest that the Cr^{+3} ions are already incorporated in the hematite lattice in the HTS-V catalyst and after activation they remain incorporated in the magnetite lattice in the HTS-A catalyst, as already observed in other activated catalysts [5,11,12].

The Cu K-edge experiments are more challenging due to its low concentration (<2%) in a dense matrix (iron oxide). Fig. 6a shows the XANES spectra where it is possible to clearly observe the Cu modification after the activation process. The spectra of reference compounds are shown in Fig. 6b.

The XANES Cu K-edge spectra for the HTS-V resemble a mixture of CuO and $Cu(OH)_2$ reference spectra whereas the HTS-A catalysts does not have a corresponding match (Fig. 6a and b). The CuO and $Cu(OH)_2$ present oxidation state II but the Cu ions occupy different sites (CuO-planar and $Cu(OH)_2$-octahedral). These results suggest that the Cu ions in the HTS-V catalyst may occupy distorted octahedral sites as a result of their incorporation in the hematite matrix, as found in other HTS catalysts [8,5]. However, it cannot be rule out that the Cu ions occupy more that one kind of geometrical site.

For the HTS-A catalyst, the data show a partial reduction of the Cu after the activation. This seems in principle to be contradictory to the literature that point out a complete reduction of the Cu after the activation process [8]. The Cu would be segregated from the magnetite particle as a metallic nanoparticle, which will be the active phase of the copper. However, it is important to mention that in this work the catalyst HTS-A was exposed to the air before the analysis and as a

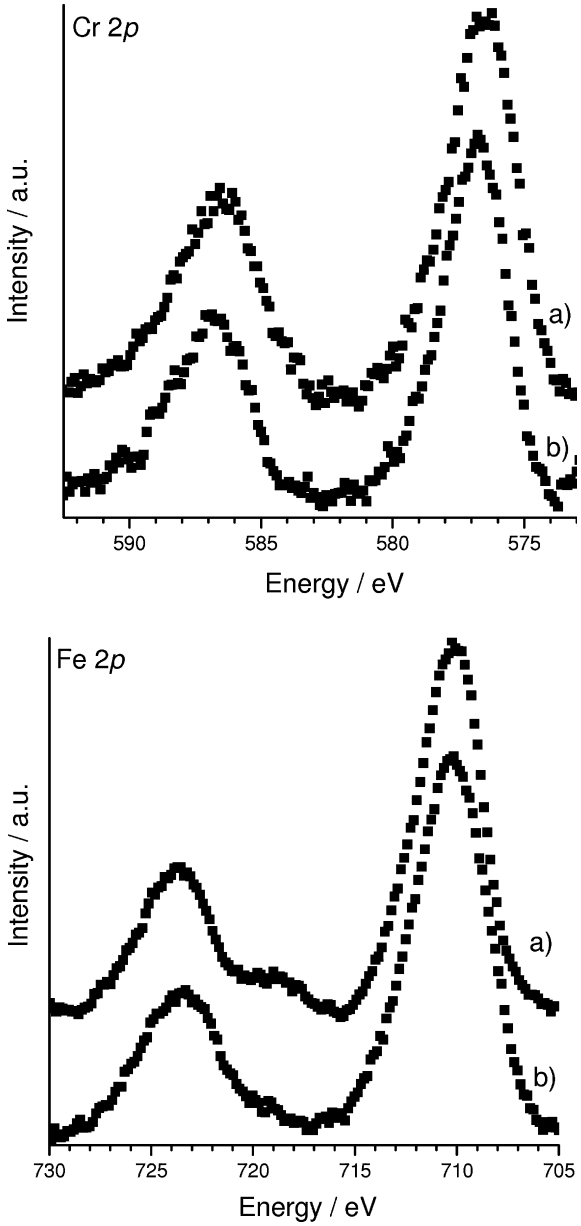

Fig. 7. Cr (top) and Fe (bottom) 2p XPS spectra for: (a) HTS-V and (b) HTS-A catalysts.

consequence, it is expected at least a partial oxidation of the Cu. In fact, it is known that CuO-based catalysts used in shift reaction are extremely susceptible to re-oxidation [22]. Hence, the mixture of oxidation states suggests the coexistence of more than one Cu species (that means not only as nanoparticle), indicating a more complex Cu activation process. Detailed *in situ* studies are planed to further address the modification of the Cu during the activation process and its role in the catalytic performance in this catalyst.

Finally, XPS analysis was performed to obtain information about the chemical composition of the catalyst surface. Fig. 7 presents the Fe 2p and Cr 2p XPS data.

The relative atomic percentages (at.%) of Cr and Fe were calculated from the XPS spectra. Cu has not been included in the analysis since we observed an undesired modification of the spectra due to the irradiation by the X-ray beam for both samples (the Cu species in the HTS-V catalyst are less sensitive to the beam when compared to the HTS-A catalyst). The Cr/Fe ratio in both HTS-V and HTS-A catalyst were the same and equal to 0.25, much larger than the nominal value (∼0.1). This corresponds to a chromium surface enrichment of more than 150%, similar to previous result in freshly activated HTS-system [5]. It has been suggested that this enrichment is an important factor to stabilize the ion oxide particles against oxidation. One of the most significant result pointed out in our analysis was that the enrichment is similar in both samples, indicating that there is no significant diffusion of the Cr ions during the bulk phase transformation from hematite to magnetite and probably increasing the stabilization of the catalyst in the very first stages. This is in agreement with the molecular modeling calculation with showed that chromium fits well into both hematite and magnetite lattices [5,23]. The chromium enrichment in the surface of HTS-system is critical because it is related to the higher thermal stability, reduces the sintering effect but also affects the intrinsic activity, as mentioned before [5,10,11,12].

4. Conclusion

In summary, we have performed a detail characterization of the activation process of a HTS catalyst using complementary techniques. We found that our catalyst presented an excellent performance that should be related to the several characteristics suggested in the literature as optimized requirements. The initial hematite phase in the HTS-V catalyst transform to magnetite phase in the HTS-A catalyst without significant loss of textural property that is probably related to the rather homogenous particle size in the HTS-V sample and the similar enrichment of Cr on particle surface in both HTS-V and HTS-A samples. These features seem to be the key points to decrease the sintering process under the WGSR conditions. The modification suffered by the Cu promoter seems to be similar to the other catalysts studied in the literature, but still remain to be fully understood. Complementary studies on the complete deactivation process are planned for better understanding of the catalyst performance and its correlation with different properties.

Acknowledgements

We are grateful to Dr. G. Azevedo (XANES), Dr. F. Garcia (XANES) and Prof. R. Landers (XPS) for fruitful discussions and suggestions. We thank Oxiteno S.A. Ind. Com. for the nitrogen adsorption and mercury porosimetry analysis and LNLS for the use of its facilities and staff support (XRD1 and XAFS beamlines, LME for the TEM experiments). MS thanks the CNPq for partial funding to participate in the LNLS 15th Summer School Program; MSPF and MHJ thank the CNPq for DTI fellowships.

References

[1] L. Lloyd, D.E. Ridler, M.V. Twigg, in: V. Martyn, Twigg (Eds.), Catalysis Handbook, Manson Publishing, England, 1996, p. 283.
[2] K. Knözinger, in: G. Ertl, H. Knözinger, J. Weitkamp (Eds.), Handbook of Heterogeneous Catalysis, vol. 4, 1997, p. 1831.
[3] M.O.G. Souza, E.B. Quadro, M.C. Rangel, Química Nova 21 (1998) 428–433.
[4] M.L. Kundu, A.C. Sengupta, G.C. Maiti, B. Sen, S.K. Ghosh, V.I. Kuznetsov, G.N. Kustova, E.N. Yurchenko, J. Catal. 112 (1988) 375–383.
[5] M.A. Edwards, D.M. Whitte, C. Rhodes, A.M. Ward, D. Rohan, M.D. Shannon, Phys. Chem. Chem. Phys. 4 (2002) 3902–3908.
[6] M.I. Markina, G.K. Koreskov, F.P. Ivanwski, L. Yudkovskaya, Kinet. Catal. 2 (1961) 867–871.
[7] C. Rhodes, G.J. Hutchings, Phys. Chem. Chem. Phys. 5 (2003) 2719–2723.
[8] P. Kappen, J.-D. Grunwaldt, B.S. Hammershoi, L. Tröger, B.S. Clausen, J. Catal. 198 (2001) 56–65.
[9] C. Rhodes, B.P. Williams, F. King, G.J. Hutchings, Catal. Commun. 3 (2002) 381–384.
[10] E.B. Quadro, M.L.R. Dias, A.M.M. Amorinm, M.C. Rangel, J. Braz. Chem. Soc. 1 (1999) 51–58.
[11] G. Doppler, A.X. Trautwein, H.M. Ziethen, E. Ambach, R. Lehnert, M.J. Sprague, U. Gonser, Appl. Catal. 40 (1988) 119–130.
[12] G.C. Chinchen, R.H. Logan, M.S. Spencer, Appl. Catal. 12 (1984) 89–96.
[13] D.A. Shirley, Phys. Rev. B 5 (1972), 4709 & 1972.
[14] http://www.casaxps.com.
[15] J.C. Gonzalez, M.G. Gonzalez, M.A. Laborde, N. Moreno, Appl. Catal. 20 (1986) 3–13.
[16] R.L. Keiski, T. Salmi, Appl. Catal. A 87 (1992) 61.
[17] J.F. Banfield, S.A. Welch, H.Z. Zhang, T.T. Ebert, R.L. Penn, Science 289 (2000) 751–754.
[18] F.G. Requejo, J.M. Ramallo-López, A.R. Beltramone, L.B. Pierella, O.A. Anunziata, Appl. Catal. A 266 (2004) 147–153.
[19] A.A. Battiston, J.H. Bitter, W.M. Heijboer, F.M.F. de Groot, D.C. Koningsberger, J. Catal. 213 (2003) 251–271.
[20] T.W. Capehart, J.F. Herbst, F.E. Pinkerton, Phys. Rev. B 52 (1995) 7907–7914.
[21] S. Takenaka, N. Hanaizumi, V.T.D. Son, K. Otsuka, J. Catal. 228 (2004) 405–416.
[22] X. Wang, J.A. Rodriguez, J.C. Hanson, D. Gamarra, A. Martínez-Arias, M. Fernández-García, J. Phys. Chem. B 1220 (2006) 428–434.
[23] J. Koy, J. Ladebeck, J.R. Hill, Stud. Surf. Sci. Catal. 119 (1998) 479.